CORE
Metadata, citation and similar papers at core.ac.uk
Provided by Elsevier - Publisher Connector

Journal of Computational and Applied Mathematics 255 (2014) 812–824

Contents lists available at ScienceDirect

Journal of Computational and Applied Mathematics

journal homepage: www.elsevier.com/locate/cam

A hybrid finite difference/control volume method for the three dimensional poroelastic wave equations in the spherical coordinate system☆,☆☆

Wensheng Zhang[a,*], Li Tong[a], Eric T. Chung[b]

[a] LSEC, Academy of Mathematics and Systems Science, Chinese Academy of Sciences, Beijing 100190, China
[b] Department of Mathematics, The Chinese University of Hong Kong, Hong Kong

ARTICLE INFO

Article history:
Received 8 November 2012
Received in revised form 11 April 2013

MSC:
35L05
65N06
65N08
65Z05

Keywords:
3D
Poroelastic wave equations
Finite difference method
Control volume method
Spherical domain
Singularity

ABSTRACT

In this paper, we consider the numerical approximation of the three-dimensional poroelastic wave equations in the spherical coordinate system. One difficulty in the design of an efficient numerical scheme is that the problem is singular in the center and the polar axes of the computational domain. Nevertheless, we develop a hybrid finite difference/control volume method for solving this problem. Our method is explicit and is second order accurate in both space and time. Numerical results are shown to confirm the convergence rate of our method and the effectiveness to simulate wave propagation in poroelastic media in the spherical coordinate system.

© 2013 The Authors. Published by Elsevier B.V. All rights reserved.

1. Introduction

The simulation of elastic wave propagation in complex poroelastic media is an important research area due to its wide range of applications in various fields such as geophysics and petroleum engineering. For instance, in order to obtain useful insight for the exploration of hydrocarbon, the behavior of elastic waves propagating in fluid-saturated porous media is crucial. Biot's linear theory [1–4] has been used as a basis for solving wave propagation problem in fluid saturated porous media. This theory is established under the following assumptions: (1) the fluid phase is continuous so that disconnected pores are treated as if a single solid matrix; (2) the porous media is statistically isotropic, which means for all cross sections, the ratio of pore area to the solid occupied area is essentially constant; (3) the microscopic pore size is much smaller than the seismic wavelength; (4) the deformations are small, which guarantees linearity of the mechanical processes; (5) the solid matrix is elastic. By using a model based on the poroelastic wave equations, the effects of fluid, pressure, porosity and permeability between phases can be systematically taken into account and provides more accurate solutions that cannot be obtained through the use of Biot's linear theory, which consists of a pure elastic or acoustic wave equation.

☆ This is an open-access article distributed under the terms of the Creative Commons Attribution–NonCommercial–No Derivative Works License, which permits non-commercial use, distribution, and reproduction in any medium, provided the original author and source are credited.

☆☆ This work is supported by the 973 State Key Project under the grant No. 2010 CB731505. It is also supported partially by the National Center for Mathematics and Interdisciplinary Sciences, Chinese Academy of Sciences.

* Corresponding author. Tel.: +86 010 62627374.
E-mail addresses: zws@lsec.cc.ac.cn (W. Zhang), tongli@lsec.cc.ac.cn (L. Tong), tschung@math.cuhk.edu.hk (E.T. Chung).

0377-0427/$ – see front matter © 2013 The Authors. Published by Elsevier B.V. All rights reserved.
http://dx.doi.org/10.1016/j.cam.2013.06.029

The finite difference method is perhaps the most popular and practical tool used in simulating acoustic and elastic wave propagation [5–11]. In literature, there are many numerical schemes for solving the Biot equations, for example, the classical finite difference schemes are developed in [12–14], the staggered-grid finite difference method in [15–18] and the discontinuous Galerkin method in [19]. All of these methods are of course based on rectangular computational domains. In some practical situations such as the wave scattering problem [20,21], the computational domain is a spherical domain or a semi-infinite half-space domain and computations in the spherical coordinate system are more suitable. Moreover, one needs to solve the poroelastic wave equations in unbounded domains, and thus one needs to impose some artificial boundary conditions. One option is the so-called exact nonreflecting boundary conditions [21–24]. The construction of such boundary conditions is based on a spherical computational domain and spherical harmonics. Hence, it is more convenient to solve the resulting problem in spherical coordinates. In this paper, we consider the numerical approximation of the three-dimensional poroelastic wave equations defined on a spherical computational domain in the spherical coordinate system. The finite difference method provides a fast and easy-to-implement numerical method for such a problem. The main difficulty in the design of an efficient numerical scheme is that the problem is singular in the center and the polar axes of the computational domain. It is the purpose of this paper to develop an efficient scheme for this problem. In particular, we will propose a hybrid finite difference/control volume method for computing a numerical solution of the problem. Our method is explicit and is second order accurate in both space and time, despite the singularities.

The paper is organized as follows. In Section 2, we will present the three dimensional poroelastic wave equations in the spherical coordinate system and the corresponding finite difference scheme in non-singular regions. Then in Section 3, we will give a control volume approach to tackle the singular region, and this is the backbone of our hybrid method. In Section 4, we present some numerical results to verify the effectiveness and the rate of convergence of our method. Finally, we give a conclusion.

2. Poroelastic wave equations in a spherical coordinate system

According to Biot's theory, wave propagation in a three dimensional statistically poroelastic medium is described by Biot equations [1–4]:

$$2\sum_j \frac{\partial}{\partial x_j}(\mu\sigma_{ij}) + \frac{\partial}{\partial x_i}(\lambda\sigma - \alpha M\xi) = \frac{\partial^2}{\partial t^2}(\rho u_i + \rho_f w_i), \tag{2.1}$$

$$\frac{\partial}{\partial x_i}(\alpha M e - M\xi) = \frac{\partial}{\partial t^2}(\rho_f u_i + \mathring{\rho} w_i) + \frac{\eta}{\kappa}\frac{\partial w_i}{\partial t}, \tag{2.2}$$

where $\mathring{\rho} = a\rho_f/\phi$ is the apparent density, and

$$M = \left(\frac{\phi}{K_f} + \frac{\alpha - \phi}{K_s}\right)^{-1}, \quad \alpha = 1 - \frac{K_b}{K_s}. \tag{2.3}$$

In Eqs. (2.1)–(2.3), the physical parameters of the medium are described as follows: μ is the shear modulus of the dry porous matrix; λ is the Lamé constant of the saturated matrix; ϕ is the porosity; κ is the permeability of the matrix; ρ is the overall density of the saturated medium given by $\rho = \phi\rho_f + (1-\phi)\rho_s$; ρ_f is the density of the pore fluid, ρ_s is the density of the solid grains; η is the viscosity of the pore fluid; a is the tortuosity of the matrix; K_s is the bulk modulus of the matrix material; K_f is the bulk modulus of the pore fluid; K_b is the bulk modulus of the dry porous frame.

The Eqs. (2.1) and (2.2) consist of six equations defined in a three dimensional medium for the six components u_i and w_i, $i = 1, 2, 3$, where u_i is the ith component of the displacement vector of the solid material, $w_i = \phi(U_i - u_i)$ is the ith component of the displacement vector of the pore fluid relative to that of the solid, and U_i is the displacement vector of the pore fluid. Moreover, $\sigma_{ij} = (\partial u_j/\partial x_i + \partial u_i/\partial x_j)/2$ is the strain tensor in the porous medium, $\xi = -\nabla\cdot\boldsymbol{w}$ is the dilatation of the relative motion between the fluid and the solid, and $e = \nabla\cdot\boldsymbol{u}$ is the dilatation of the solid motion.

Now we consider a spherical computational domain $\mathcal{B}$ centered at the origin with radius R and assume that the medium is homogeneous. We will need to represent a vector field in spherical coordinates. For a general vector field $\boldsymbol{f}(r,\vartheta,\phi,t)$, we use f^r, f^ϑ and f^ϕ to represent the components of $\boldsymbol{f}$ in the directions $\hat{\boldsymbol{r}}$, $\hat{\boldsymbol{\vartheta}}$ and $\hat{\boldsymbol{\phi}}$ respectively, where $\hat{\boldsymbol{r}}$, $\hat{\boldsymbol{\vartheta}}$ and $\hat{\boldsymbol{\phi}}$ are the unit vectors in the spherical coordinate system. Let $\boldsymbol{u} = (u^r, u^\vartheta, u^\phi, t)$ and $\boldsymbol{w} = (w^r, w^\vartheta, w^\phi, t)$. Then in the spherical coordinate system, Eqs. (2.1) and (2.2) can be written as:

$$\begin{aligned}(\mathring{\rho}\rho - \rho_f^2)\frac{\partial^2 u^r}{\partial t^2} &= (\mathring{\rho}\lambda + \mathring{\rho}\mu - \alpha\rho_f M)\frac{\partial}{\partial r}\Big(G(u^r, u^\theta, u^\phi)\Big) \\ &\quad + (\alpha\mathring{\rho}M - \rho_f M)\frac{\partial}{\partial r}\Big(G(w^r, w^\theta, w^\phi)\Big) + \mathring{\rho}\mu H(u^r) + \frac{\eta\rho_f}{\kappa}\frac{\partial w^r}{\partial t},\end{aligned} \tag{2.4}$$

$$\begin{aligned}(\mathring{\rho}\rho - \rho_f^2)\frac{\partial^2 u^\vartheta}{\partial t^2} &= \frac{(\mathring{\rho}\lambda + \mathring{\rho}\mu - \alpha\rho_f M)}{r}\frac{\partial}{\partial\vartheta}\Big(G(u^r, u^\vartheta, u^\phi)\Big) \\ &\quad + \frac{(\alpha\mathring{\rho}M - \rho_f M)}{r}\frac{\partial}{\partial\vartheta}\Big(G(w^r, w^\vartheta, w^\phi)\Big) + \mathring{\rho}\mu\Big(H(u^\vartheta)\Big) + \frac{\eta\rho_f}{\kappa}\frac{\partial w^\vartheta}{\partial t},\end{aligned} \tag{2.5}$$

$$
\begin{aligned}
(\mathring{\rho}\rho-\rho_f^2)\frac{\partial^2 u^\phi}{\partial t^2} \;=\;& \frac{(\mathring{\rho}\lambda+\mathring{\rho}\mu-\alpha\rho_f M)}{r\sin\vartheta}\frac{\partial}{\partial\phi}\Big(G(u^r,u^\vartheta,u^\phi)\Big)\\
&+\frac{(\alpha\mathring{\rho}M-\rho_f M)}{r\sin\vartheta}\frac{\partial}{\partial\phi}\Big(G(w^r,w^\vartheta,w^\phi)\Big)+\mathring{\rho}\mu\Big(H(u^\phi)\Big)+\frac{\eta\rho_f}{\kappa}\frac{\partial w^\phi}{\partial t},
\end{aligned}
\tag{2.6}
$$

$$
\begin{aligned}
(\mathring{\rho}\rho-\rho_f^2)\frac{\partial^2 w^r}{\partial t^2} \;=\;& (\alpha\rho M-\rho_f\lambda-\rho_f\mu)\frac{\partial}{\partial r}\Big(G(u^r,u^\vartheta,u^\phi)\Big)\\
&+(\rho M-\alpha\rho_f M)\frac{\partial}{\partial r}\Big(G(w^r,w^\vartheta,w^\phi)\Big)-\rho_f\mu\Big(H(u^r)\Big)-\frac{\eta\rho}{\kappa}\frac{\partial w^r}{\partial t},
\end{aligned}
\tag{2.7}
$$

$$
\begin{aligned}
(\mathring{\rho}\rho-\rho_f^2)\frac{\partial^2 w^\vartheta}{\partial t^2} \;=\;& \frac{(\alpha\rho M-\rho_f\lambda-\rho_f\mu)}{r}\frac{\partial}{\partial\vartheta}\Big(G(u^r,u^\vartheta,u^\phi)\Big)\\
&+\frac{(\rho M-\alpha\rho_f M)}{r}\frac{\partial}{\partial\vartheta}\Big(G(w^r,w^\vartheta,w^\phi)\Big)-\rho_f\mu\Big(H(u^\vartheta)\Big)-\frac{\eta\rho}{\kappa}\frac{\partial w^\vartheta}{\partial t},
\end{aligned}
\tag{2.8}
$$

$$
\begin{aligned}
(\mathring{\rho}\rho-\rho_f^2)\frac{\partial^2 w^\phi}{\partial t^2} \;=\;& \frac{(\alpha\rho M-\rho_f\lambda-\rho_f\mu)}{r\sin\vartheta}\frac{\partial}{\partial\phi}\Big(G(u^r,u^\vartheta,u^\phi)\Big)\\
&+\frac{(\rho M-\alpha\rho_f M)}{r\sin\vartheta}\frac{\partial}{\partial\phi}\Big(G(w^r,w^\vartheta,w^\phi)\Big)-\rho_f\mu\Big(H(u^\phi)\Big)-\frac{\eta\rho}{\kappa}\frac{\partial w^\phi}{\partial t},
\end{aligned}
\tag{2.9}
$$

where G and H are defined by

$$
G(f^r,f^\vartheta,f^\phi):=\frac{\partial f^r}{\partial r}+\frac{2f^r}{r}+\frac{1}{r}\frac{\partial f^\vartheta}{\partial\vartheta}+\frac{\cos\vartheta}{r\sin\vartheta}f^\vartheta+\frac{1}{r\sin\vartheta}\frac{\partial f^\phi}{\partial\phi},
\tag{2.10}
$$

$$
H(f^r):=\frac{\partial^2 f^r}{\partial r^2}+\frac{2}{r}\frac{\partial f^r}{\partial r}+\frac{\cos\vartheta}{r^2\sin\vartheta}\frac{\partial f^r}{\partial\vartheta}+\frac{1}{r^2}\frac{\partial^2 f^r}{\partial\vartheta^2}+\frac{1}{r^2\sin^2\vartheta}\frac{\partial^2 f^r}{\partial\phi^2},
\tag{2.11}
$$

respectively.

A grid is defined on the computational domain $\mathscr{B}$ by using the mesh sizes $\Delta r=R/N_r$, $\Delta\vartheta=\pi/N_\vartheta$ and $\Delta\phi=2\pi/N_\phi$ in the directions $\hat{\boldsymbol{r}}$, $\hat{\boldsymbol{\vartheta}}$ and $\hat{\boldsymbol{\phi}}$ respectively. The value of the component $u^r(r,\vartheta,\phi,t)$ at a general grid point and at a time $n\Delta t$ is denoted by $u^r_{(i,j,k,n)}$, where Δt is the time step and $i=0,1,2,\ldots,N_r$; $j=0,1,\ldots,N_\vartheta$; $k=0,1,\ldots,N_\phi-1$. Furthermore, to simplify the notations, we sometimes write $u^r_{(i,j,k,n)}=u^r$ in the difference scheme. Similar notations are also used for the other components u^ϑ, u^ϕ, w^r, w^ϑ and w^ϕ. In the following, we will consider the discretization of (2.4)–(2.9) in the non-singular regions. These regions correspond to grid points with indices $i\neq 0$ and $j\neq 0, N_\vartheta$. The discretization in the singular region will be discussed in the next section.

For ease of notation, we write the second-order central difference operators as

$$
\begin{cases}
\delta_t^2 f:=f_{(i,j,k,n+1)}-2f_{(i,j,k,n)}+f_{(i,j,k,n-1)},\\
\delta_r^2 f:=f_{(i+1,j,k,n)}-2f_{(i,j,k,n)}+f_{(i-1,j,k,n)},\\
\delta_\vartheta^2 f:=f_{(i,j+1,k,n)}-2f_{(i,j,k,n)}+f_{(i,j-1,k,n)},\\
\delta_\phi^2 f:=f_{(i,j,k+1,n)}-2f_{(i,j,k,n)}+f_{(i,j,k-1,n)},
\end{cases}
\tag{2.12}
$$

the first-order central difference operators as

$$
\begin{cases}
\delta_r f:=f_{(i+1,j,k,n)}-f_{(i-1,j,k,n)},\\
\delta_\vartheta f:=f_{(i,j+1,k,n)}-f_{(i,j-1,k,n)},\\
\delta_\phi f:=f_{(i,j,k+1,n)}-f_{(i,j,k-1,n)},
\end{cases}
\tag{2.13}
$$

and the first-order forward difference operators as

$$
\begin{cases}
\gamma_r f:=f_{(i+1,j,k,n)}-f_{(i,j,k,n)},\\
\gamma_\vartheta f:=f_{(i,j+1,k,n)}-f_{(i,j,k,n)},\\
\gamma_\phi f:=f_{(i,j,k+1,n)}-f_{(i,j,k,n)}.
\end{cases}
\tag{2.14}
$$

Using these operators, we can construct a second order finite-difference scheme for the system (2.4)–(2.9) at any grid point with indices i,j,k satisfying $i=1,2\ldots,N_r-1$, $j=1,2\ldots,N_\vartheta-1$ and $k=0,1\ldots,N_\phi-1$. For instance, the discretization of (2.4) is given by

$$
\begin{aligned}
u^r_{(i,j,k,n+1)}=2u^r_{(i,j,k,n)}-u^r_{(i,j,k,n-1)}+\frac{(\mathring{\rho}\lambda+\mathring{\rho}\mu-\alpha\rho_f M)\Delta t^2}{\mathring{\rho}\rho-\rho_f^2}\Bigg\{\frac{1}{(\Delta r)^2}\left(\delta_r^2+\frac{2\gamma_r}{i}-\frac{2}{i^2}\right)u^r\\
+\frac{1}{2i\Delta\vartheta(\Delta r)^2}\left(\gamma_r\delta_\vartheta-\frac{\delta_\vartheta}{i}\right)u^\vartheta+\frac{1}{i(\Delta r)^2}\left(\frac{\cos j\Delta\vartheta}{i\sin j\Delta\vartheta}\gamma_r-\frac{1}{i}\right)u^\vartheta
\end{aligned}
$$

$$+\frac{1}{2i(\Delta r)^2\Delta\phi}\left(\frac{\gamma_r\delta_\phi}{\sin j\Delta\vartheta}-\frac{\delta_\phi}{i}\right)u^\phi\Bigg\}+\frac{(\alpha\mathring{\rho}M-\rho_f M)\Delta t^2}{\mathring{\rho}\rho-\rho_f^2}\Bigg\{\frac{1}{(\Delta r)^2}\left(\delta_r^2+\frac{2\gamma_r}{i}-\frac{2}{i^2}\right)w^r$$
$$+\frac{1}{2i\Delta\vartheta(\Delta r)^2}\left(\gamma_r\delta_\vartheta-\frac{\delta_\vartheta}{i}\right)w^\vartheta+\frac{\cos j\Delta\vartheta}{i(\Delta r)^2\sin j\Delta\vartheta}\left(\gamma_r-\frac{1}{i}\right)w^\vartheta$$
$$+\frac{1}{2i(\Delta r)^2\Delta\phi}\frac{1}{\sin j\Delta\vartheta}\left(\gamma_r\delta_\phi-\frac{1}{i}\delta_\vartheta\right)w^\phi\Bigg\}$$
$$+\frac{\mathring{\rho}\mu\Delta t^2}{\mathring{\rho}\rho-\rho_f^2}\Bigg\{\frac{1}{(\Delta r)^2}\left(\delta_r^2+\frac{2\gamma_r}{i}\right)u^r+\frac{\cos j\Delta\vartheta}{\sin j\Delta\vartheta}\frac{1}{2\Delta\vartheta(i\Delta r)^2}\delta_r u^r$$
$$+\frac{1}{(i\Delta r)^2(\Delta\vartheta)^2}\left(\delta_\vartheta^2+\frac{\delta_\phi^2}{(\sin j\Delta\vartheta)^2}\right)u^r\Bigg\}+\frac{\eta\rho_f\Delta t}{2\kappa}\left(w^r_{(i,j,k,n+1)}-w^r_{(i,j,k,n-1)}\right). \tag{2.15}$$

The discretization for the Eqs. (2.5)–(2.9) can be derived in a similar way.

3. Discretization in singular regions

The discretization by using classical second order finite difference discussed in the previous section cannot be applied in singular regions for the system (2.4)–(2.9). These singular regions include the center of the spherical computational domain ($r=0$) and the polar axes ($\vartheta=0,\pi$). In this section, we propose a control volume approach [25] to overcome this difficulty.

3.1. Discretization at the center $r=0$

In this section, we will present the discretization for the three dimensional poroelastic wave equations at the sphere center $r=0$. We will provide the discretization of (2.4) for u^r in detail, the discretization for the other Eqs. (2.5)–(2.9) can be constructed similarly. First, we integrate (2.4) on a sphere with radius $\Delta r/2$ and center at $r=0$. Then, using the midpoint rule for the left hand side (LHS) of the resulting equation, we obtain the following discretization:

$$\begin{aligned}\text{LHS} &= (\mathring{\rho}\rho-\rho_f^2)\int_0^{2\pi}\int_0^{\pi}\int_0^{\Delta r/2}\frac{\partial^2 u^r}{\partial t^2}r^2\sin\vartheta\, dr d\vartheta d\phi\\ &\approx (\mathring{\rho}\rho-\rho_f^2)\frac{\partial^2 u^r}{\partial t^2}\Big|_{r=0}\int_0^{2\pi}\int_0^{\pi}\int_0^{\Delta r/2} r^2\sin\vartheta\, dr d\vartheta d\phi\\ &\approx \frac{\pi(\mathring{\rho}\rho-\rho_f^2)\Delta r^3}{6\Delta t^2}\delta_t^2 u^r_{(0,j,k,n)}.\end{aligned} \tag{3.1}$$

The right hand side (RHS) of the resulting equation contains three integral terms, and we give the approximation for each of them in the following. The first integral on the RHS is

$$\begin{aligned}&\int_0^{2\pi}\int_0^{\pi}\int_0^{\Delta r/2}\frac{\partial}{\partial r}\left(\frac{\partial u^r}{\partial r}+\frac{2u^r}{r}+\frac{1}{r}\frac{\partial u^\vartheta}{\partial\vartheta}+\frac{\cos\vartheta}{r\sin\vartheta}u^\vartheta+\frac{1}{r\sin\vartheta}\frac{\partial u^\phi}{\partial\phi}\right)r^2\sin\vartheta\, dr d\vartheta d\phi\\ &=\int_0^{2\pi}\int_0^{\pi}\Bigg[\left(\frac{\partial u^r}{\partial r}+\frac{2u^r}{r}+\frac{1}{r}\frac{\partial u^\vartheta}{\partial\vartheta}+\frac{\cos\vartheta}{r\sin\vartheta}u^\vartheta+\frac{1}{r\sin\vartheta}\frac{\partial u^\phi}{\partial\phi}\right)r^2\sin\vartheta\Big|_{r=0}^{\Delta r/2}\\ &\quad-\int_0^{\Delta r/2}\left(\frac{\partial u^r}{\partial r}+\frac{2u^r}{r}+\frac{1}{r}\frac{\partial u^\vartheta}{\partial\vartheta}+\frac{\cos\vartheta}{r\sin\vartheta}u^\vartheta+\frac{1}{r\sin\vartheta}\frac{\partial u^\phi}{\partial\phi}\right)2r\sin\vartheta\, dr\Bigg]d\vartheta d\phi.\end{aligned} \tag{3.2}$$

Observe that $\frac{\partial u^r}{\partial r}+\frac{2u^r}{r}=\frac{1}{r^2}\frac{\partial(r^2u^r)}{\partial r}$ and $\frac{1}{r}\frac{\partial u^\vartheta}{\partial\vartheta}+\frac{\cos\vartheta}{r\sin\vartheta}u^\vartheta=\frac{1}{r\sin\vartheta}\frac{\partial(\sin\vartheta u^\vartheta)}{\partial\vartheta}$, we can then approximate each term in (3.2) involving the r-derivative as follows:

$$\begin{aligned}\int_0^{2\pi}\int_0^{\pi}\frac{\partial(r^2u^r)}{\partial r}\sin\vartheta\Big|_{r=\Delta r/2}d\vartheta d\phi &\approx \int_0^{2\pi}\int_0^{\pi}\frac{r^2u^r\,|_{r=\Delta r}-r^2u^r\,|_{r=0}}{\Delta r}\sin\vartheta\, d\vartheta d\phi\\ &\approx \Delta r\int_0^{2\pi}\int_0^{\pi}u^r_{(1,j,k,n)}\sin\vartheta\, d\vartheta d\phi\\ &\approx \Delta r\Delta\vartheta\Delta\phi\sum_{j=1}^{N_\vartheta-1}\sum_{k=0}^{N_\phi-1}u^r_{(1,j,k,n)}\sin j\Delta\vartheta,\end{aligned} \tag{3.3}$$

where the trapezoidal rule is used in last approximation, and

$$\int_0^{2\pi}\int_0^{\pi}\int_0^{\Delta r/2}\frac{2\sin\vartheta}{r}\frac{\partial(r^2u^r)}{\partial r}drd\vartheta d\phi = 2\int_0^{2\pi}\int_0^{\pi}\sin\vartheta\left(ru^r\ |_0^{\Delta r/2}+\int_0^{\Delta r/2}u^r dr\right)d\vartheta d\phi$$
$$\approx\frac{\Delta r\Delta\vartheta\Delta\phi}{4}\sum_{j=1}^{N_\vartheta-1}\sum_{k=0}^{N_\phi-1}\left(5u^r_{(0,j,k,n)}+3u^r_{(1,j,k,n)}\right)\sin j\Delta\vartheta. \tag{3.4}$$

The other terms in (3.2) can be computed as follows:

$$\int_0^{2\pi}\int_0^{\pi}\left.\frac{\partial(\sin\vartheta u^\vartheta)}{\partial\vartheta}r\right|_{r=\Delta r/2}d\vartheta d\phi = 0, \tag{3.5}$$

$$\int_0^{2\pi}\int_0^{\pi}\left.\frac{\partial u^\phi}{\partial\phi}r\right|_{r=\Delta r/2}d\vartheta d\phi = 0, \tag{3.6}$$

$$\int_0^{2\pi}\int_0^{\pi}\int_0^{\Delta r/2}\frac{\partial(\sin\vartheta u^\vartheta)}{\partial\vartheta}drd\vartheta d\phi = 0, \tag{3.7}$$

$$\int_0^{2\pi}\int_0^{\pi}\int_0^{\Delta r/2}\frac{\partial u^\phi}{\partial\phi}drd\vartheta d\phi = 0. \tag{3.8}$$

Therefore the first integral of RHS can be approximated by

$$\int_0^{2\pi}\int_0^{\pi}\int_0^{\Delta r/2}\frac{\partial}{\partial r}\left(\frac{\partial u^r}{\partial r}+\frac{2u^r}{r}+\frac{1}{r}\frac{\partial u^\vartheta}{\partial\vartheta}+\frac{\cos\vartheta}{r\sin\vartheta}u^\vartheta+\frac{1}{r\sin\vartheta}\frac{\partial u^\phi}{\partial\phi}\right)r^2\sin\vartheta drd\vartheta d\phi$$
$$\approx\frac{\Delta r\Delta\vartheta\Delta\phi}{4}\sum_{j=1}^{N_\vartheta-1}\sum_{k=0}^{N_\phi-1}\left(u^r_{(1,j,k,n)}-5u^r_{(0,j,k,n)}\right)\sin j\Delta\vartheta. \tag{3.9}$$

Similarly, for the second integral of RHS, we have the following approximation

$$\int_0^{2\pi}\int_0^{\pi}\int_0^{\Delta r/2}\frac{\partial}{\partial r}\left(\frac{\partial w^r}{\partial r}+\frac{2w^r}{r}+\frac{1}{r}\frac{\partial w^\vartheta}{\partial\vartheta}+\frac{\cos\vartheta}{r\sin\vartheta}w^\vartheta+\frac{1}{r\sin\vartheta}\frac{\partial w^\phi}{\partial\phi}\right)r^2\sin\vartheta drd\vartheta d\phi$$
$$\approx\frac{\Delta r\Delta\vartheta\Delta\phi}{4}\sum_{j=1}^{N_\vartheta-1}\sum_{k=0}^{N_\phi-1}\left(w^r_{(1,k,j,n)}-5w^r_{(0,j,k,n)}\right)\sin j\Delta\vartheta. \tag{3.10}$$

For the third integral of RHS:

$$\int_0^{2\pi}\int_0^{\pi}\int_0^{\Delta r/2}\left(r^2\frac{\partial^2u^r}{\partial r^2}+2r\frac{\partial u^r}{\partial r}+\frac{\cos\vartheta}{\sin\vartheta}\frac{\partial u^r}{\partial\vartheta}+\frac{\partial^2u^r}{\partial\vartheta^2}+\frac{1}{\sin^2\vartheta}\frac{\partial^2u^r}{\partial\phi^2}\right)\sin\vartheta drd\vartheta d\phi, \tag{3.11}$$

the term involving r-derivative can be approximated by

$$\int_0^{2\pi}\int_0^{\pi}\int_0^{\Delta r/2}\frac{\partial}{\partial r}\left(r^2\frac{\partial u^r}{\partial r}\right)\sin\vartheta drd\vartheta d\phi = \frac{(\Delta r)^2}{4}\int_0^{2\pi}\int_0^{\pi}\left.\frac{\partial u^r}{\partial r}\right|_{r=\Delta r/2}\sin\vartheta d\vartheta d\phi \tag{3.12}$$
$$\approx\frac{\Delta r\Delta\vartheta\Delta\phi}{4}\sum_{j=1}^{N_\vartheta-1}\sum_{k=0}^{N_\phi-1}\left(u^r_{(1,j,k,n)}-u^r_{(0,j,k,n)}\right)\sin j\Delta\vartheta, \tag{3.13}$$

and the other terms can be computed as follows:

$$\int_0^{2\pi}\int_0^{\pi}\int_0^{\Delta r/2}\frac{\partial}{\partial\vartheta}\left(\sin\vartheta\frac{\partial u^r}{\partial\vartheta}\right)drd\vartheta d\phi = 0, \tag{3.14}$$

$$\int_0^{2\pi}\int_0^{\pi}\int_0^{\Delta r/2}\frac{1}{\sin\vartheta}\frac{\partial^2u^r}{\partial\phi^2}drd\vartheta d\phi = 0. \tag{3.15}$$

Thus the third integral of RHS can be approximated by

$$\int_0^{2\pi}\int_0^{\pi}\int_0^{\Delta r/2}\left(r^2\frac{\partial^2 u^r}{\partial r^2}+2r\frac{\partial u^r}{\partial r}+\frac{\cos\vartheta}{\sin\vartheta}\frac{\partial u^r}{\partial\vartheta}+\frac{\partial^2 u^r}{\partial\vartheta^2}+\frac{1}{\sin^2\vartheta}\frac{\partial^2 u^r}{\partial\phi^2}\right)\sin\vartheta\, dr d\vartheta d\phi$$
$$\approx\frac{\Delta r\Delta\vartheta\Delta\phi}{4}\sum_{j=1}^{N_\vartheta-1}\sum_{k=0}^{N_\phi-1}\left(u^r_{(1,j,k,n)}-u^r_{(0,j,k,n)}\right)\sin j\Delta\vartheta. \tag{3.16}$$

Combining the above results in (3.1), (3.9), (3.10) and (3.16), we obtain a numerical scheme for u^r at the sphere center $r=0$:

$$\begin{aligned}u^r_{(0,j,k,n+1)} &= 2u^r_{(0,j,k,n)}-u^r_{(0,j,k,n-1)}+\frac{3\Delta t^2\Delta\vartheta\Delta\phi(\mathring{\rho}\lambda+\mathring{\rho}\mu-\alpha\rho_f M)}{2\pi(\Delta r)^2(\mathring{\rho}\rho-\rho_f^2)}\\ &\quad\times\sum_{j=1}^{N_\vartheta-1}\sum_{k=0}^{N_\phi-1}\left(u^r_{(1,j,k,n)}-5u^r_{(0,j,k,n)}\right)\sin j\Delta\vartheta+\frac{3\Delta t^2\Delta\vartheta\Delta\phi(\alpha\mathring{\rho}M-\rho_f M)}{2\pi(\Delta r)^2(\mathring{\rho}\rho-\rho_f^2)}\\ &\quad\times\sum_{j=1}^{N_\vartheta-1}\sum_{j=0}^{N_\phi-1}\left(w^r_{(1,j,k,n)}-5w^r_{(0,j,k,n)}\right)\sin j\Delta\vartheta+\frac{3\Delta t^2\Delta\vartheta\Delta\phi\mathring{\rho}\mu}{2\pi(\Delta r)^2(\mathring{\rho}\rho-\rho_f^2)}\\ &\quad\times\sum_{j=1}^{N_\vartheta-1}\sum_{k=0}^{N_\phi-1}\left(u^r_{(1,j,k,n)}-u^r_{(0,j,k,n)}\right)\sin j\Delta\vartheta+\frac{\eta\rho_f\Delta t}{2\kappa}\left(w^r_{(0,j,k,n+1)}-w^r_{(0,j,k,n-1)}\right).\end{aligned}\tag{3.17}$$

The approximation of (2.5)–(2.6) at the sphere center $r=0$ can be derived in a similar way. Integrating on both sides of (2.5) with $\int_0^{2\pi}\int_0^{\pi}\int_0^{\Delta r/2}r^2\sin^2\vartheta\, dr\delta\vartheta d\phi$ and making further approximation, we can obtain the difference scheme of (2.5) for u^ϑ at $r=0$:

$$\begin{aligned}u^\vartheta_{(0,j,k,n+1)} &= 2u^\vartheta_{(0,j,k,n)}-u^\vartheta_{(0,j,k,n-1)}+\frac{(\mathring{\rho}\lambda+\mathring{\rho}\mu-\alpha\rho_f M)\Delta t^2}{(\mathring{\rho}\rho-\rho_f^2)S_1}\left\{-\frac{\Delta r\Delta\vartheta\Delta\phi}{8}\sum_{j=1}^{N_\vartheta-1}\sum_{k=0}^{N_\phi-1}\left[3u^r_{(1,j,k,n)}\sin(2j\Delta\vartheta)\right.\right.\\ &\quad\left.\left.+2\big(3u^\vartheta_{(0,j,k,n)}+u^\vartheta_{(1,j,k,n)}\big)\sin^2(j\Delta\vartheta)\right]\right\}+\frac{(\alpha\mathring{\rho}M-\rho_f M)\Delta t^2}{(\mathring{\rho}\rho-\rho_f^2)S_1}\\ &\quad\times\left\{-\frac{\Delta r\Delta\vartheta\Delta\phi}{8}\sum_{j=1}^{N_\vartheta-1}\sum_{k=0}^{N_\phi-1}\left[3w^r_{(1,j,k,n)}\sin(2j\Delta\vartheta)+2\big(3w^\vartheta_{(0,j,k,n)}+w^\vartheta_{(1,j,k,n)}\big)\sin^2(j\Delta\vartheta)\right]\right\}\\ &\quad+\frac{\mathring{\rho}\mu\Delta t^2}{(\mathring{\rho}\rho-\rho_f^2)S_1}\left\{\frac{\Delta r\Delta\vartheta\Delta\phi}{8}\sum_{j=1}^{N_\vartheta-1}\sum_{k=0}^{N_\phi-1}\left[2\big(u^\vartheta_{(1,j,k,n)}-u^\vartheta_{(0,j,k,n)}\big)\sin^2(j\Delta\vartheta)\right.\right.\\ &\quad\left.\left.+u^\vartheta_{(1,j,k,n)}\cos 2j\Delta\vartheta\right]+\frac{\pi\Delta r\Delta\vartheta}{8}\left(u^\vartheta_{(1,0,0,n)}+u^\vartheta_{(1,N_\vartheta,0,n)}\right)\right\}+\frac{\eta\rho_f\Delta t}{2\kappa}\left(w^\vartheta_{(0,j,k,n+1)}-w^\vartheta_{(0,j,k,n-1)}\right).\end{aligned}\tag{3.18}$$

The discretization of (2.6) for u^ϕ can be obtained like that of (2.4), and the result is

$$\begin{aligned}u^\phi_{(0,j,k,n+1)} &= 2u_{(0,j,k,n)}-u_{(0,j,k,n-1)}+\frac{\mathring{\rho}\mu\Delta t^2}{(\mathring{\rho}\rho-\rho_f^2)S_2}\left\{\frac{\Delta r\Delta\vartheta\Delta\phi}{4}\sum_{j=1}^{N_\vartheta-1}\sum_{k=0}^{N_\phi-1}\left(u^\phi_{(1,j,k,n)}-u^\phi_{(0,j,k,n)}\right)\sin j\Delta\vartheta\right\}\\ &\quad+\frac{\eta\rho_f\Delta t}{2\kappa}\left(w^\phi_{(0,j,k,n+1)}-w^\phi_{(0,j,k,n-1)}\right),\end{aligned}\tag{3.19}$$

where $S_1=\pi^2\Delta r^3/24$ and $S_2=\pi\Delta r^3/6$. Finally, we remark that the approximation of (2.7)–(2.9) for $\boldsymbol{w}$ at the sphere center $r=0$ can be derived like $\boldsymbol{u}$ as above, and we omit the details.

3.2. Discretization along polar axes $\vartheta=0$ and $\vartheta=\pi$

In this section, we will present the discretization of (2.4)–(2.9) along the polar axes $\vartheta=0$ and $\vartheta=\pi$ by a control volume approach. We will give the discretization for (2.4) along $\vartheta=0$ in detail since the discretization along $\vartheta=\pi$ is similar. We integrate both sides of (2.4) on a spherical cap with height $r(1-\cos(\Delta\vartheta/2))$. The resulting LHS can be approximated by

$$\mathrm{LHS}=(\mathring{\rho}\rho-\rho_f^2)\int_0^{2\pi}\int_0^{\Delta\vartheta/2}\frac{\partial^2 u^r}{\partial t^2}r^2\sin\vartheta\, d\vartheta d\phi\approx\frac{(\mathring{\rho}\rho-\rho_f^2)S}{\Delta t^2}\delta_t^2 u^r_{(i,0,k,n)},\tag{3.20}$$

where $S = 2\pi r^2(1 - \cos\Delta\vartheta/2)$ is the area of the spherical cap. The RHS of the resulting equation contains three integrals. We will approximate each of them as follows. The first integral of RHS is given by

$$\int_0^{2\pi}\int_0^{\Delta\vartheta/2}\frac{\partial}{\partial r}\left(\frac{\partial u^r}{\partial r}+\frac{2u^r}{r}+\frac{1}{r}\frac{\partial u^\vartheta}{\partial\vartheta}+\frac{\cos\vartheta}{r\sin\vartheta}u^\vartheta+\frac{1}{r\sin\vartheta}\frac{\partial u^\phi}{\partial\phi}\right)r^2\sin\vartheta\,d\vartheta\,d\phi. \tag{3.21}$$

The first four terms in (3.21) can be approximated by using

$$\int_0^{2\pi}\int_0^{\Delta\vartheta/2}\frac{\partial}{\partial r}\left(\frac{\partial u^r}{\partial r}\right)r^2\sin\vartheta\,d\vartheta\,d\phi\approx\frac{S}{(\Delta r)^2}\delta_r^2u^r_{(i,0,k,n)}, \tag{3.22}$$

$$\int_0^{2\pi}\int_0^{\Delta\vartheta/2}\frac{\partial}{\partial r}\left(\frac{u^r}{r}\right)r^2\sin\vartheta\,d\vartheta\,d\phi\approx\frac{S}{(\Delta r)^2}\left(\frac{\gamma_r}{i}-\frac{1}{i^2}\right)u^r_{(i,0,k,n)}, \tag{3.23}$$

and

$$\begin{aligned}\int_0^{2\pi}\int_0^{\Delta\vartheta/2}\frac{\partial}{\partial r}\left(\frac{1}{r\sin\vartheta}\frac{\partial(\sin\vartheta u^\vartheta)}{\partial\vartheta}\right)r^2\sin\vartheta\,d\vartheta\,d\phi &\approx \frac{\Delta\phi\sin(\Delta\vartheta/2)}{2}\sum_{k=0}^{N_\phi-1}\left(iu^\vartheta_{(i+1,1,k,n)}-(i+1)u^\vartheta_{(i,1,k,n)}\right)\\ &\quad+i\pi\sin(\vartheta/2)u^\vartheta_{(i+1,0,k,n)}-(i+1)\pi\sin(\vartheta/2)u^\vartheta_{(i,0,k,n)},\end{aligned} \tag{3.24}$$

where in the last approximation we have used $\frac{1}{r}\frac{\partial u^\vartheta}{\partial\vartheta}+\frac{\cos\vartheta}{r\sin\vartheta}u^\vartheta=\frac{1}{r\sin\vartheta}\frac{\partial(\sin\vartheta u^\vartheta)}{\partial\vartheta}$. For the last term in (3.21), we have

$$\int_0^{2\pi}\int_0^{\Delta\vartheta/2}\frac{\partial}{\partial r}\left(\frac{1}{r\sin\vartheta}\frac{\partial u^\phi}{\partial\phi}\right)r^2\sin\vartheta\,d\vartheta\,d\phi=0. \tag{3.25}$$

Combining (3.22)–(3.25), we obtain an approximation of (3.21). Next we consider the second integral of RHS

$$\int_0^{2\pi}\int_0^{\Delta\vartheta/2}\left(\frac{\partial^2u^r}{\partial r^2}+\frac{2}{r}\frac{\partial u^r}{\partial r}+\frac{\cos\vartheta}{r^2\sin\vartheta}\frac{\partial u^r}{\partial u^\vartheta}+\frac{1}{r^2}\frac{\partial^2u^r}{\partial\vartheta^2}+\frac{1}{r^2\sin^2\vartheta}\frac{\partial^2u^r}{\partial\phi^2}\right)r^2\sin\vartheta\,d\vartheta\,d\phi, \tag{3.26}$$

which can be approximated based on the following expressions:

$$\int_0^{2\pi}\int_0^{\Delta\vartheta/2}\left(\frac{\partial^2u^r}{\partial r^2}+\frac{2}{r}\frac{\partial u^r}{\partial r}\right)r^2\sin\vartheta\,d\vartheta\,d\phi\approx S\left[\frac{\delta_r^2}{(\Delta r)^2}+\frac{2\gamma_r}{i\Delta r^2}\right]u^r_{(i,0,k,n)},$$

$$\int_0^{2\pi}\int_0^{\Delta\vartheta/2}\frac{\partial}{\partial\vartheta}\left(\sin\vartheta\frac{\partial u^r}{\partial\vartheta}\right)d\vartheta\,d\phi\approx\frac{\sin(\Delta\vartheta/2)}{\Delta\vartheta}\left[\Delta\phi\sum_{k=0}^{N_\phi-1}u^r_{(i,1,k,n)}-2\pi u^r_{(i,0,k,n)}\right],$$

and

$$\int_0^{2\pi}\int_0^{\Delta\vartheta/2}\left(\frac{1}{\sin\vartheta}\frac{\partial^2u^r}{\partial\phi^2}\right)d\vartheta\,d\phi=0.$$

Combining all the above results, the discretization of (2.4) for u^r along the polar axis $\vartheta = 0$ is

$$\begin{aligned}u^r_{(i,0,k,n+1)} &= 2u^r_{(i,0,k,n)}-u^r_{(i,0,k,n-1)}+\frac{(\mathring{\rho}\lambda+\mathring{\rho}\mu-\alpha\rho_fM)\Delta t^2}{\mathring{\rho}\rho-\rho_f^2}\Bigg\{\frac{1}{(\Delta r)^2}\left(\delta_r^2+\frac{2\gamma_r}{i}-\frac{2}{i^2}\right)u^r_{(i,0,k,n)}\\ &\quad+\frac{\Delta\phi\sin(\Delta\vartheta/2)}{2S}\sum_{k=0}^{N_\phi-1}\left[iu^\vartheta_{(i+1,1,k,n)}-(i+1)u^\vartheta_{(i,1,k,n)}\right]+\frac{\pi\sin(\vartheta/2)}{S}\left[iu^\vartheta_{(i+1,0,k,n)}-(i+1)u^\vartheta_{(i,0,k,n)}\right]\Bigg\}\\ &\quad+\frac{(\alpha\mathring{\rho}M-\rho_fM)\Delta t^2}{\mathring{\rho}\rho-\rho_f^2}\Bigg\{\frac{1}{(\Delta r)^2}\left(\delta_r^2+\frac{2\delta_r}{i}-\frac{2}{i^2}\right)w^r_{(i,0,k,n)}+\frac{\Delta\phi\sin(\Delta\vartheta/2)}{2S}\\ &\quad\times\sum_{k=0}^{N_\phi-1}\left[iu^\vartheta_{(i+1,1,k,n)}-(i+1)u^\vartheta_{(i,1,k,n)}\right]+\frac{\pi\sin(\vartheta/2)}{S}\left[iu^\vartheta_{(i+1,0,k,n)}-(i+1)u^\vartheta_{(i,0,k,n)}\right]\Bigg\}\\ &\quad+\frac{\mathring{\rho}\mu\Delta t^2}{\mathring{\rho}\rho-\varrho_f^2}\Bigg\{\frac{1}{(\Delta r)^2}\left(\delta_r^2-\frac{2\delta_r}{i}\right)u^r_{(i,0,k,n)}+\frac{\sin(\Delta\vartheta/2)}{S\Delta\vartheta}\left[\Delta\phi\sum_{k=0}^{N_\phi-1}u^r_{(i,1,k,n)}-2\pi u^r_{(i,0,k,n)}\right]\Bigg\}\\ &\quad+\frac{\eta\rho\Delta t}{2\kappa}\left(w^r_{(i,0,k,n+1)}-w^r_{(i,0,k,n-1)}\right).\end{aligned} \tag{3.27}$$

The discretizations of (2.5)–(2.6) for u^{ϑ} and u^{ϕ} along $\vartheta = 0$ can also be obtained. The resulting schemes are the following expression ($i = 1, \ldots, N_r - 1$):

$$\begin{aligned} u^{\vartheta}_{(i,0,k,n+1)} &= 2u^{\vartheta}_{(i,0,k,n)} - u^{\vartheta}_{(i,0,k,n-1)} + \frac{(\mathring{\rho}\lambda + \mathring{\rho}\mu - \alpha\rho_f M)\Delta t^2}{(\mathring{\rho}\rho - \rho_f^2)S_3}\left\{A\left[\Delta\phi\sum_{k=0}^{N_\phi-1}\left(\frac{i}{2}u^r_{(i+1,i,k,n)} + \left(1-\frac{i}{2}\right)u^r_{(i,1,k,n)}\right)\right.\right. \\ &\quad \left.\left. + i\pi u_{(i+1,0,k,n)} + (2-i)\pi u^r_{(i,0,k,n)}\right] + D\sum_{k=0}^{N_\phi-1} u^{\vartheta}_{(i,1,k,n)} - 2\pi B u^{\vartheta}_{(i,0,k,n)}\right\} \\ &\quad + \frac{(\alpha\mathring{\rho}M - \rho_f M)\Delta t^2}{(\mathring{\rho}\rho - \rho_f^2)S_3}\left\{A\left[\Delta\phi\sum_{k=0}^{N_\phi-1}\left(\frac{i}{2}w^r_{(i+1,i,k,n)} + \left(1-\frac{i}{2}\right)w^r_{(i,1,k,n)}\right)\right.\right. \\ &\quad \left.\left. + i\pi w_{(i+1,0,k,n)} + (2-i)\pi w^r_{(i,0,k,n)}\right] + D\sum_{k=0}^{N_\phi-1} w^{\vartheta}_{(i,1,k,n)} - 2\pi B w^{\vartheta}_{(i,0,k,n)}\right\} \\ &\quad + \frac{\mathring{\rho}\mu\Delta t^2}{(\mathring{\rho}\rho - \rho_f^2)S_3}\left\{\frac{S_3}{(\Delta r)^2}\left(\frac{2\gamma_r}{i} + \delta_r^2\right)u^{\vartheta}_{(i,j,k,n)} + C\left[\Delta\phi\sum_{k=0}^{N_\phi-1} u^{\vartheta}_{(i,1,k,n)} - 2\pi u^{\vartheta}_{(i,0,k,n)}\right]\right\} \\ &\quad + \frac{\eta\rho\Delta t}{2\kappa}\left(w^{\vartheta}_{(i,0,k,n+1)} - w^{\vartheta}_{(i,0,k,n-1)}\right), \end{aligned} \tag{3.28}$$

$$\begin{aligned} u^{\phi}_{(i,0,k,n+1)} &= 2u^{\phi}_{(i,0,k,n)} - u^{\phi}_{(i,0,k,n-1)} + \frac{\mathring{\rho}\mu\Delta t^2}{(m\rho - \rho_f^2)S_4}\left\{\frac{S_4}{(\Delta r)^2}\left(\delta_r^2 + \frac{2\gamma_r}{i}\right)u^{\phi}_{(i,j,k,n)}\right. \\ &\quad \left. + \frac{\sin(\Delta\vartheta/2)\Delta\phi}{\Delta\vartheta}\sum_{k=0}^{N_\phi-1} u^{\phi}_{(i,1,k,n)} - \frac{2\pi\sin(\Delta\vartheta/2)}{\Delta\vartheta}u^{\phi}_{(i,0,k,n)}\right\} + \frac{\eta\rho\Delta t}{2\kappa}\left(w^{\phi}_{(i,0,k,n+1)} - w^{\phi}_{(i,0,k,n-1)}\right), \end{aligned} \tag{3.29}$$

where A, B, C and D are given by

$$\begin{aligned} A &= \sin^2\frac{\Delta\vartheta}{2} - \Delta\vartheta\sin\frac{\Delta\vartheta}{2}\cos\frac{\Delta\vartheta}{2}, \\ B &= \frac{\sin(\Delta\vartheta/2)\sin\Delta\vartheta}{\Delta\vartheta} - \sin\frac{\Delta\vartheta}{2}\cos\frac{\Delta\vartheta}{2} - \frac{\Delta\vartheta}{4}\sin^2\frac{\Delta\vartheta}{2}, \\ C &= \frac{1}{\Delta\vartheta}\sin^2\frac{\Delta\vartheta}{2} - \frac{\sin\Delta\vartheta}{8}, \\ D &= \frac{\sin(\Delta\vartheta/2)\sin\Delta\vartheta}{\Delta\vartheta} - \sin\frac{\Delta\vartheta}{2}\cos\frac{\Delta\vartheta}{2} - \frac{\Delta\vartheta}{4}\sin^2\frac{\Delta\vartheta}{2}, \end{aligned} \tag{3.30}$$

respectively, and

$$S_3 = \pi r^2\left(\frac{\Delta\vartheta}{2} - \frac{\sin\Delta\vartheta}{2}\right), \qquad S_4 = 2\pi r^2\left(1 - \cos\frac{\Delta\vartheta}{2}\right). \tag{3.31}$$

We remark that (3.28) is derived based on making integration on both sides of (2.5) with $\int_0^{2\pi}\int_0^{\Delta\vartheta/2} r^2\sin^2\vartheta\, d\vartheta\, d\phi$. This is different from the derivation of (3.27) or (3.29) where we make integration with $\int_0^{2\pi}\int_0^{\Delta\vartheta/2} r^2\sin\vartheta\, d\vartheta\, d\phi$ on both sides of (2.4) or (2.6).

The discretization of (2.4) for u^r along $\vartheta = \pi$ can be derived similarly if we integrate both sides of (2.4) with $\int_0^{2\pi}\int_{\pi-\Delta\vartheta/2}^{\pi} r^2\sin\vartheta\, d\vartheta\, d\phi$. The final result is the following:

$$\begin{aligned} u^r_{(i,N_\vartheta,k,n+1)} &= 2u^r_{(i,N_\vartheta,k,n)} - u^r_{(i,N_\vartheta,k,n-1)} + \frac{(\mathring{\rho}\lambda + \mathring{\rho}\mu - \alpha\rho_f M)\Delta t^2}{\mathring{\rho}\rho - \rho_f^2}\left\{\frac{1}{(\Delta r)^2}\left(\delta_r^2 + \frac{2\gamma_r}{i} - \frac{2}{i^2}\right)u^r_{(i,N_\vartheta,k,n)}\right. \\ &\quad - \frac{\Delta\phi\sin(\Delta\vartheta/2)}{2S_4}\sum_{k=0}^{N_\phi-1}\left[iu^{\vartheta}_{(i+1,N_\vartheta-1,k,n)} + (i+1)u^{\vartheta}_{(i,N_\vartheta-1,k,n)}\right] - \frac{\pi\sin(\vartheta/2)}{S_4} \\ &\quad \left.\times\left[iu^{\vartheta}_{(i+1,N_\vartheta,k,n)} - (i+1)u^{\vartheta}_{(i,N_\vartheta,k,n)}\right]\right\} + \frac{(\alpha\mathring{\rho}M - \rho_f M)\Delta t^2}{\mathring{\rho}\rho - \rho_f^2}\left\{\frac{1}{(\Delta r)^2}\left(\delta_r^2 + \frac{2\delta_r}{i} - \frac{2}{i^2}\right)w^r_{(i,N_\vartheta,k,n)}\right. \\ &\quad - \frac{\Delta\phi\sin(\Delta\vartheta/2)}{2S_4}\sum_{k=0}^{N_\phi-1}\left[iu^{\vartheta}_{(i+1,N_\vartheta-1,k,n)} - (i+1)u^{\vartheta}_{(i,N_\vartheta-1,k,n)}\right] \end{aligned}$$

$$-\frac{\pi\sin(\vartheta/2)}{S_4}\left[iu^{\vartheta}_{(i+1,N_\vartheta,k,n)}-(i+1)u^{\vartheta}_{(i,N_\vartheta,k,n)}\right]\Bigg\}+\frac{\mathring{\rho}\mu\Delta t^2}{\mathring{\rho}\rho-\varrho_f^2}\left\{\frac{1}{(\Delta r)^2}\left(\delta_r^2+\frac{2\delta_r}{i}\right)u^r_{(i,N_\vartheta,k,n)}\right.$$
$$\left.+\frac{\sin(\Delta\vartheta/2)}{S_4\Delta\vartheta}\left[\Delta\phi\sum_{k=0}^{N_\phi-1}u^r_{(i,N_\vartheta-1,k,n)}-2\pi u^r_{(i,N_\vartheta,k,n)}\right]\right\}+\frac{\eta\rho\Delta t}{2\kappa}\left(w^r_{(i,N_\vartheta,k,n+1)}-w^r_{(i,N_\vartheta,k,n-1)}\right). \tag{3.32}$$

The difference schemes of (2.5) for u^θ along $\vartheta=\pi$ is

$$\begin{aligned}u^{\theta}_{(i,N_\theta,k,n+1)}&=2u^{\theta}_{(i,N_\theta,k,n)}-u^{\theta}_{(i,N_\theta,k,n-1)}+\frac{(\mathring{\rho}\lambda+\mathring{\rho}\mu-\alpha\rho_f M)\Delta t^2}{(\mathring{\rho}\rho-\rho_f^2)S_3}\left\{-A\left[\sum_{k=0}^{N_\phi-1}\left(\frac{(i+1)^2}{2i}u^r_{(i+1,N_\theta-1,k,n)}\right.\right.\right.\\&\left.\left.-\frac{i}{2}u^r_{(i,N_\theta-1,k,n)}\right)+\frac{(i+1)^2}{i}\pi u^r_{(i+1,N_\theta,k,n)}-i\pi u^r_{(i,N_\theta,k,n)}\right]+E\left[\frac{1}{2}\sum_{k=0}^{N_\phi-1}u^{\theta}_{(i,N_\theta-1,k,n)}+\pi u^{\theta}_{(r,N_\theta,k,n)}\right]\Bigg\}\\&+\frac{(\alpha\mathring{\rho}M-\rho_f M)\Delta t^2}{(\mathring{\rho}\rho-\rho_f^2)S_3}\left\{-A\left[\sum_{k=0}^{N_\phi-1}\left(\frac{(i+1)^2}{2i}w^r_{(i+1,N_\theta-1,k,n)}-\frac{i}{2}w^r_{(i,N_\theta-1,k,n)}\right)\right.\right.\\&\left.+\frac{(i+1)^2}{i}\pi w^r_{(i+1,N_\theta,k,n)}-i\pi w^r_{(i,N_\theta,k,n)}\right]+E\left[\frac{1}{2}\sum_{k=0}^{N_\phi-1}w^{\theta}_{(i,N_\theta-1,k,n)}+\pi w^{\theta}_{(i,N_\theta,k,n)}\right]\Bigg\}\\&+\frac{\mathring{\rho}\mu\Delta t^2}{(\mathring{\rho}\rho-\rho_f^2)S_3}\left\{\frac{S_3}{\Delta r^2}\delta_r^2u^{\theta}_{(i,N_\theta,k,n)}+\frac{2S_3}{i\Delta r^2}\gamma_r u^{\theta}_{(i,N_\theta,k,n)}+F\left[2\pi u^{\theta}_{(i,N_\theta,k,n)}-\sum_{k=0}^{N_\phi-1}u^{\theta}_{(i,N_\theta-1,k,n)}\Delta\phi\right]\right\}\\&+\frac{\eta\rho\Delta t}{2\kappa}\left(w^{\vartheta}_{(i,N_\vartheta,k,n+1)}-w^{\vartheta}_{(i,N_\vartheta,k,n-1)}\right),\end{aligned} \tag{3.33}$$

and the difference scheme of (2.6) for u^ϕ along $\vartheta=\pi$ is

$$\begin{aligned}u^{\phi}_{(i,N_\theta,k,n+1)}&=2u^{\phi}_{(i,N_\theta,k,n)}-u^{\phi}_{(i,N_\theta,k,n-1)}+\frac{\mathring{\rho}\mu\Delta t^2}{(\mathring{\rho}\rho-\rho_f^2)S_3}\left\{\frac{S_3}{\Delta r^2}\delta_r^2u^{\phi}_{(i,N_\theta,k,n)}+\frac{2}{i\Delta r^2S_3}\gamma_r u^{\phi}_{(i,N_\theta,k,n)}\right.\\&\left.+F\left[2\pi u^{\phi}_{(i,N_\theta,k,n)}-\sum_{k=0}^{N_\phi-1}u^{\phi}_{(i,N_\theta-1,k,n)}\Delta\phi\right]\right\}+\frac{\eta\rho\Delta t}{2\kappa}\left(w^{\phi}_{(i,N_\vartheta,k,n+1)}-w^{\phi}_{(i,N_\vartheta,k,n-1)}\right),\end{aligned} \tag{3.34}$$

where

$$E=\frac{2\sin^2\frac{\Delta\theta}{2}}{\Delta\theta}-\sin\Delta\theta,\qquad F=\frac{\frac{\Delta\theta}{8}\sin\Delta\theta-\sin^2\frac{\Delta\theta}{2}}{\Delta\theta}. \tag{3.35}$$

We remark that the derivation of (3.33) is based on integration on both sides of (2.5). We omit the schemes of (2.7)–(2.9) for $\boldsymbol{w}$ along $\vartheta=0$ and π for saving space as they can be derived in the same way. In computations, we need to compute $\boldsymbol{w}^{n+1}$ first and then compute $\boldsymbol{u}^{n+1}$.

4. Numerical results

In this section we will present numerical results to illustrate the convergence of our numerical method. In our computations, we choose $N_r=40$, $N_\vartheta=40$, $N_\phi=40$, and $\Delta t=0.0001$ s. The radius R is fixed at 500 m. The source function is defined as

$$f=\delta(r-r_0,\vartheta-\vartheta_0,\phi-\phi_0)(\sin(50t)e^{-1000t^2},0,0), \tag{4.1}$$

where $(r_0,\vartheta_0,\phi_0)=(0,0,0)$ is the position of the source. The dynamic behavior is provided by Biot's theory which predicts two compressional waves and one shear wave [1–4]. The CFL stability condition used in our computations is [7,26]

$$\frac{\Delta t}{\Delta r}\le\frac{1}{\sqrt{C_{p_1}^2+C_{p_2}^2+C_s^2}}. \tag{4.2}$$

The three velocities C_{p1}, C_{p2} and C_s can be obtained from the physical parameters of the porous medium.

In our simulations, the three velocities are chosen as $C_{p_1}=2360$ m/s, $C_{p_2}=775$ m/s and $C_s=960$ m/s. This choice requires that $\Delta t/\Delta r$ is not more than about 0.00038 s/m. The other physical parameters are listed in Table 4.1. The dimension of K_f, K_s, K_b and μ is 10^{10} Pa. In computations the permeability is 1.0×10^{-12} m^2. The boundary conditions

Table 4.1
Physical properties of the model used in numerical computations.

K_f	ρ_f (kg/m^3)	Ks	ρ_s (kg/m^3)	K_b	μ	a	η (Pa s)
2.4	1040	3.5	2650	4.17	1.855	2167	0.001

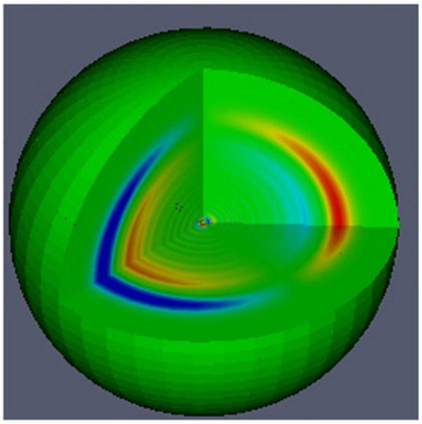

Fig. 4.1. 3D snapshot of the component u_x at propagation time $t = 0.12$ s.

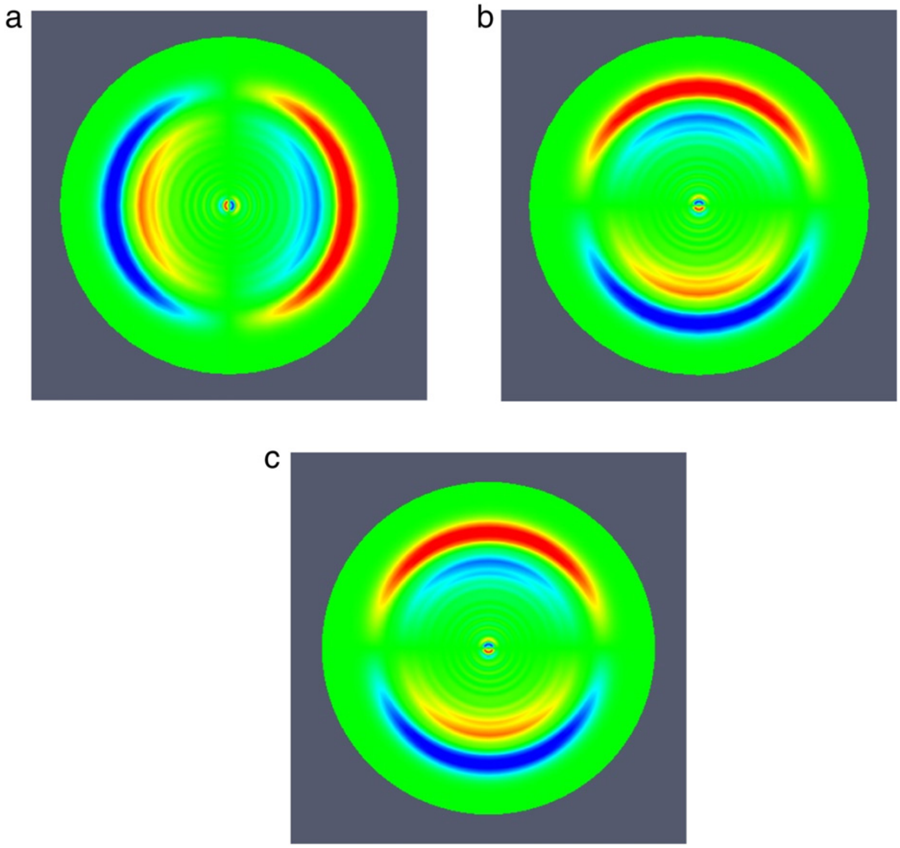

Fig. 4.2. Snapshot sections through the center of the sphere at propagation time $t = 0.12$ s. (a) The section of u_x along z direction; (b) The section of u_y along z direction; (c) The section of u_z along x direction.

used in our computations are the Dirichlet boundary conditions. We stop waves from reaching the boundary and focus on the effectiveness of our hybrid method. For absorbing boundary conditions in poroelastic media, the reader can refer to the references, for example, [14,16,18,24]. The computed components in spherical coordinates are usually transformed into

Table 4.2
Numerical L_2 errors of the computed results with various meshes while the mesh ratios are unchanged.

$Nr \times N_\vartheta \times N_\phi$	L_2 norm errors
12 × 12 × 12	3.400e−06
18 × 18 × 18	1.444e−06
24 × 24 × 24	7.660e−07
30 × 30 × 30	4.543e−07
36 × 36 × 36	2.856e−07
42 × 42 × 42	1.842e−07
48 × 48 × 48	1.186e−07
54 × 54 × 54	7.366e−08

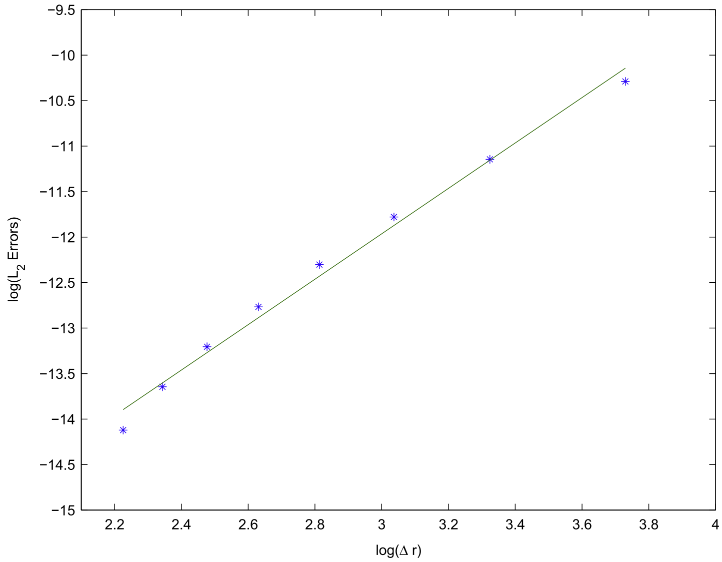

Fig. 4.3. A log–log plot for the L_2 norm errors.

Table 4.3
Numerical L_2 errors of the computed results with various time steps while grids points N_r, N_ϑ and N_ϕ are all fixed 24.

Δt (s)	L_2 norm errors
0.00500	9.044e−06
0.00400	5.775e−06
0.00200	1.437e−06
0.00100	3.579e−07
0.00050	8.871e−08
0.00025	2.150e−08
0.00020	1.343e−08
0.00010	2.686e−09

those in Cartesian coordinates for waveform analysis. The transform, for example, from $(u_r, u_\vartheta, u_\phi)$ to (u_x, u_y, u_z) is the following:

$$\begin{cases} u_x = u_r \sin\vartheta \cos\phi + u_\vartheta \cos\vartheta \cos\phi - u_\phi \sin\phi, \\ u_y = u_r \sin\vartheta \sin\phi + u_\vartheta \cos\vartheta \sin\phi + u_\phi \cos\phi, \\ u_z = u_r \cos\theta - u_\vartheta \sin\vartheta, \end{cases} \tag{4.3}$$

which is an orthogonal transform. Fig. 4.1 is the 3D snapshot of the component u_x at propagation time $t = 0.12$ s. The 3D snapshots of components u_y and u_z are omitted here for space. In Fig. 4.2, we present the sections of 3D snapshots of $\boldsymbol{u} = (u_x, u_y, u_z)$ through the center of the sphere. Fig. 4.2(a) and (b) are the sections of u_x and u_y along z direction respectively. Fig. 4.2(c) is the section of u_z along x direction. We note that three such sections, i.e., the section of u_x along x direction, the section of u_y along y direction and the section of u_z along z direction, have zero values. This is consistent with the physical phenomena. From these results we see that the waveform of solutions of $\boldsymbol{u} = (u_x, u_y, u_z)$ and the fronts of three waves are very clear.

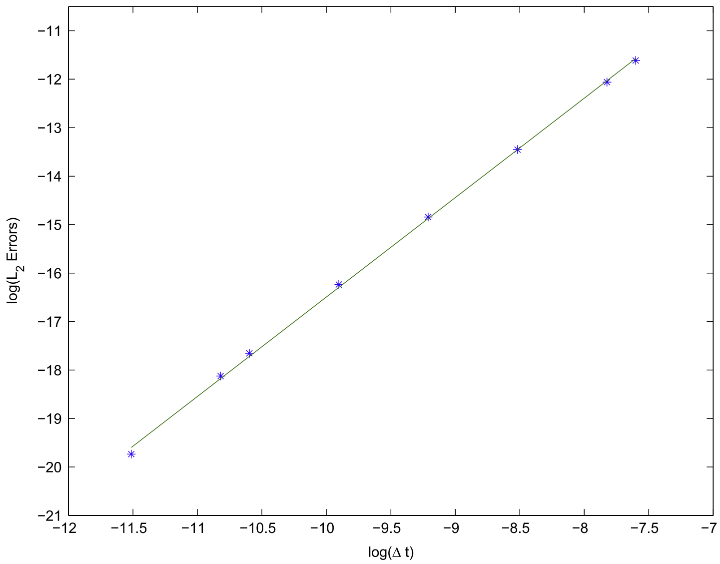

Fig. 4.4. A log–log plot for the L_2 norm errors.

In the following, we will numerically test the convergence rate of our method. In these calculations, we consider the L_2 errors with various mesh sizes. To compute the errors, a reference solution is obtained on a fine grid defined by $N_r = N_\vartheta = N_\phi = 72$. The grid ratios, i.e., $\Delta t/\Delta r$, $\Delta t/\Delta\vartheta$ and $\Delta t/\Delta\phi$, are fixed $1/24 \times 10^{-3}$ in computations. In Table 4.2, we show the L_2 errors with various mesh sizes and in Fig. 4.3, we show a log–log plot of the errors. In Fig. 4.3, the stars represent errors and the blue line represents the least square fitted line. We found that the slope of the line is 2.496. Thus we can expect a second order convergence rate in space. Next we verify the convergence rate in time. We fix $N_r = N_\vartheta = N_\phi = 24$ and use a different time step. The reference solution is obtained with $\Delta t = 5.0 \times 10^{-6}$ s on the same mesh. In Table 4.3, we give the L_2 errors with various time steps and in Fig. 4.4, we show a log–log plot of the errors. The slope of the least square fitted line in Fig. 4.4 is 2.051, which shows the rate of convergence in time is 2. Thus our hybrid method has second order accuracy both in space and time, which coincides with the theoretical facts. The numerical examples presented here are for a homogeneous media. As regards future research for the poroelastic wave equations in a heterogeneous medium and the potential interface problem may refer to exciting works for elliptic and parabolic problems, for example, [27–31].

5. Conclusions

We propose a new hybrid scheme for the three dimensional poroelastic wave equations in the spherical coordinate system. The resulting problem is defined on a spherical computational domain and singularities occur at the sphere center $r = 0$ and along the polar axes $\vartheta = 0, \pi$. To tackle this difficulty, we propose a hybrid finite difference/control volume approach. Our scheme is explicit and is second-order accurate both in space and time. Numerical results are shown to verify the convergence rate. The scheme also can be applied to the medium with piecewise constant parameter. The idea of our hybrid method can also be used to handle other elastic and acoustic wave equations.

Acknowledgments

The authors are grateful to the anonymous referees for many constructive comments that have led to a much improved presentation of the paper. We also would like to thank professors J. Hong, Z. Chen, J. Xu and J. Zou for their valuable help in the research.

References

[1] M.A. Biot, Theory of propagation of elastic waves in a fluid-saturated porous solid, I. Low-frequency range, J. Acoust. Soc. Am. 28 (1956) 168–178.
[2] M.A. Biot, Theory of propagation of elastic waves in a fluid-saturated porous solid, II. Higher-frequency range, J. Acoust. Soc. Am. 28 (1956) 179–191.
[3] M.A. Biot, Mechanics deformation and acoustic propagation in porous media, J. Appl. Phys. 33 (1962) 1482–1498.
[4] M.A. Biot, Generalized theory of acoustic propagation in porous dissipative media, J. Acoust. Soc. Am. 34 (1962) 1254–1264.
[5] R.M. Alford, K.R. Kelly, D.M. Boore, Accuracy of finite-difference modeling of acoustic wave equations, Geophysics 39 (1974) 834–841.
[6] G. Cohen, P. Joly, Construction and analysis of fourth-order finite difference schemes for the acoustic wave equation in nonhomogeneous media, SIAM J. Numer. Anal. 4 (1996) 1266–1302.
[7] G. Cohen, Higher-Order Numerical Methods for Transient Wave Equations, Springer-Verlag, 2002.
[8] S.E. Minkoff, Spatial parallelism of a 3D finite difference velocity–stress elastic wave propagation code, SIAM J. Sci. Comput. 24 (2002) 1–19.
[9] A. Sei, A family of numerical schemes for the computation of elastic waves, SIAM J. Sci. Comput. 16 (1995) 898–916.

[10] J. Virieux, P-SV wave propagation in heterogeneous media: velocity–stress finite-difference method, Geophysics 51 (1986) 889–901.
[11] W. Zhang, L. Tong, Eric T. Chung, A new high accuracy locally one-dimensional scheme for the wave equation, J. Comput. Appl. Math. 236 (2011) 1343–1353.
[12] S. Hassanzadeh, Acoustic modeling in fluid saturated porous media, Geophysics 56 (1991) 424–435.
[13] F. Wenzlau, T.M. Müller, Finite-difference modeling of wave propagation and diffusion in poroelastic media, Geophysics 74 (2009) T55–T66.
[14] Y.Q. Zeng, J.Q. He, Q.L. Liu, The application of the perfectly matched layer in numerical modeling of wave propagation in poroelastic media, Geophysics 66 (2001) 1258–1266.
[15] N. Dai, A. Vafidis, E.R. Kanasewich, Wave propagation in heterogeneous, porous media: a velocity–stress, finite-difference method, Geophysics 60 (1995) 327–340.
[16] R. Martin, D. Komatitsch, A. Ezziani, An unsplit convolutional perfectly matched layer improved at grazing incidence for seismic wave propagation in poroelastic media, Geophysics 73 (2008) T51–T61.
[17] T. Özdenvar, G.A. McMechan, Algorithms for staggered-grid computations for poroelastic, elastic, acoustic, and scalar wave equations, Geophys. Prospect. 45 (1997) 403–420.
[18] Y.Q. Zeng, Q.L. Liu, A staggered-grid finite-difference method with perfectly matched layers for poroelastic wave equations, J. Acoust. Soc. Am. 109 (2001) 2571–2580.
[19] J. de la Puente, M. Dumbser, M. Käser, H. Igel, Discontinuous Galerkin methods for wave propagation in poroelastic media, Geophysics 73 (2008) T77–T97.
[20] A. Bermúdez, L. Hervella-nieto, A. Prieto, R. Rodríguez, An exact bounded perfectly matched layer for time-harmonic scattering problems, SIAM J. Sci. Comput. 30 (2007) 312–338.
[21] L. Ting, J. Miksis, Exact boundary conditions for scattering problems, J. Acoust. Soc. Am. 80 (1986) 1825–1827.
[22] M.J. Grote, J.B. Keller, Exact nonreflecting boundary conditions for the time dependent wave equation, SIAM J. Appl. Math. 55 (1995) 280–3297.
[23] M.J. Grote, J.B. Keller, Exact nonreflecting boundary conditions for elastic waves, SIAM J. Appl. Math. 60 (2000) 803–819.
[24] W. Zhang, L. Tong, Eric T. Chung, Exact nonreflecting boundary conditions for three dimensional poroelastic wave equations, Commun. Math. Sci. 12 (2014) 59–96.
[25] J.W. Thomas, Numerical Partial Differential Equations: Finite Difference Methods, Springer-Verlag, New York, Inc., 1995.
[26] R. Courant, K.O. Friedrichs, H. Lewy, Uber die Partiellen Differenzengleichungen der Mathematischen Physik, Math. Ann. 100 (1928) 32–74.
[27] Z. Chen, J. Zou, Finite element methods and their convergence for elliptic and parabolic interface problems, Numer. Math. 79 (1998) 175–202.
[28] R. Hiptmair, J. Li, J. Zou, Convergence analysis of finite element methods for $H(\text{crul}; \Omega)$-elliptic interface problems, Numer. Math. 122 (2012) 557–578.
[29] R. Hiptmair, J. Li, J. Zou, Universal extension for Sobolev spaces of differential forms and applications, J. Funct. Anal. 263 (2012) 364–382.
[30] R. Hiptmair, J. Li, J. Zou, Convergence analysis of finite element methods for $H(\text{div}; \Omega)$-elliptic interface problems, J. Numer. Math. 18 (2010) 187–218.
[31] J. Li, J.M. Melenk, B. Wohlmuth, J. Zou, Optimal a priori estimates for higher order finite elements for elliptic interface problems, Appl. Numer. Math. 60 (2010) 19–37.